Građevinski materijali i konstrukcije
Building Materials and Structures

journal homepage: www.dimk.rs

Technical paper

Numerical thermal performance analysis of light steel insulated walls under fire

Mohammed Hassoune [*1)], Abdelhak Kada[2)], Belkacem Menadi[3)], Belkacem Lamri[4)]

[1)] *Laboratory of Geo-Materials and Civil Engineering, Department of Civil Engineering, University of Blida1, P.O.Box 270 Soumaa Road, Blida, Algeria*
[1)] *Laboratory Fire Safety Engineering of Constructions and Protection of their Environment LISICPE, Department of Civil Engineering, Hassiba Benbouali University of Chlef, B.P 78C N19 Road Ouled Fares, Chlef, Algeria*
[2)] *Laboratory of Geo-Materials and Civil Engineering, Department of Civil Engineering, University of Blida1, P.O.Box 270 Soumaa Road, Blida, Algeria*
[3)] *Laboratory Fire Safety Engineering of Constructions and Protection of their Environment LISICPE, Department of Civil Engineering, Hassiba Benbouali University of Chlef, B.P 78C N19 Road Ouled Fares, Chlef, Algeria*

A B S T R A C T

Light-gauge steel-framed (LSF) walls are being adopted by the Algerian construction industry as a new alternative to the traditional infilled frames due to the advantages they provide. The strength-to-weight ratio of Cold Formed Section (CFS) leads to lighter structures and a decrease in the building cost. However, in the case of fire, the high shape factor combined with the loss of material properties of the unprotected, slender CFS can result in structural failure. Because of their conductivity, elevated temperatures have an effect on the thermal performance of panels, necessitating the use of appropriate insulation. The purpose of this paper is to perform a numerical analysis of the thermal behavior of LSF walls protected by plasterboard or magnesium oxide board, as well as cavity insulations. Numerical models are developed, using ANSYS software to simulate the thermal performance of LSF walls under ISO 834 fire. Thermal simulations are done to predict temperature profiles, maximum temperatures, and the estimated fire resistance level (FRL). This research has produced results to better evaluate the influence of different systems of protection and insulation used for the CFS under fire.

1   Introduction

Nowadays, the use of a Light Gauge Steel Framed (LSF) wall system as a new type of structural element is benefiting the rapid expansion of building construction in Algeria. The ease of transportation and rapidity of execution have made it possible to adopt it as a new alternative building solution, especially in seismic regions, to reduce the weight of the structure. These wall systems consist of two elements of cold-formed steel (CFS), namely stud and track sections characterized by very thin sections which may restrict the use of the LSF for a non-load-bearing wall. These slender sections have better durability and a higher strength-to-weight ratio compared to hot rolled steel [1], due to the different fabrication processes that have a significant influence on mechanical material properties [2]. In a fire situation, steel material having a high thermal conductivity is vulnerable due to the loss of its mechanical properties [3, 4]. Therefore, a fire safety must be ensured as one of the important requirements that a building has to include according to contemporary technical rules on structural engineering [5]. To study the collapse of structures under elevated temperatures, most research has been done on

unprotected hot-rolled structural elements [6-10] or protected structural elements [11-13]. The structural behaviour of CFS structures under fire is complex and requires substantial, dedicated research on isolated element frames as well as on complete walls and panels. Some studies have proposed various parameters that have a significant influence on the behavior of LSF walls in terms of improving fire resistance by incorporating some protective materials [14]. Different single or double layers of wallboard can be used on both sides of the LSF wall, such as plasterboard, magnesium oxide board (MGO) and Cork [15-19]. Furthermore, using rockwool and glass fiber to form a new composite innovative panel, cavity insulation, or external insulation sandwiched between two layers of protection wallboards, could be achieved [20, 21]. Previous research has been conducted to investigate the thermal performance of LSF walls when subjected to fire, including experimental studies and numerical simulation. According to experimental studies done by Kolarkar and Mahendran [22] and Baleshan and Mahendran [23], the measured temperatures across the composite wall panel show a higher fire performance than the conventionally built non-load-bearing wall models. Keerthan and Mahendran [24], developed a numerical model of a composite LSF wall

---

[*]   Corresponding author:
   E-mail address: hassoune.mohammed@etu.univ-blida.dz

panel, protected by double layers of plasterboard and externally insulated under various thicknesses and densities using Eurocode design fire curves [25]. They concluded that using rockwool improved fire resistance significantly more than other insulation, particularly when sandwiched between double plasterboard. Ariyanayagam and Mahendran [26] also conducted an experimental study to investigate the effect of calcium silicate boards and plasterboard on non-load-bearing LSF walls exposed to fire. The results show that both wallboards provided nearly the same thermal response. Ariyanayagam and Mahendran [27] investigated, experimentally and numerically, the influence of cavity insulation on the fire resistance of non-load-bearing and load-bearing LSF walls. Their results allow for the conclusion that the FRL of cavity insulated non-load bearing LSF walls increases by more than 10 minutes, whereas it is significantly reduced for the other walls. Khetata et al. [28] performed full-scale standard fire tests, followed by a thermal modelling of composite non-load-bearing LSF, using different configurations for several protection materials and insulations. It was concluded that the increase in the number of studs and the thickness of the protection layers will enhance the fire performance, and the use of super-wool insulation provides a higher fire resistance than rockwool. Rajanayagam et al. [29] have conducted a numerical analysis to investigate the thermal performance of LSF walls and study the effect of novel thermal insulation materials. Rahnavard et al. [30] presented a 2D numerical model of heat transfer analysis with the aim of providing a new analytical formulation for the prediction of the temperature evolution within the concrete-filled cold-formed steel section (CF-CFS) when subjected to fire. It is worth mentioning that extensive research has tackled the problem of the behaviour of CFS at ambient temperature, and there is a need for more studies and investigations at elevated temperatures to enhance their fire safety. Most studies that investigated the behaviour of LSF in a fire situation, have been carried out using plasterboard as layer protection, however, the MGO layer protection, recently introduced in Algeria, requires investigation under fire conditions. Besides, there is a need for more research on the fire performance of LSF wall systems built with such layer protection and added cavity insulation within the panels. To understand the thermal response, finite element heat transfer models for different configurations of LSF wall systems exposed to ISO 834 fire have been developed. The results obtained aim to identify

the LSF wall system with improved fire resistance. Four configurations of composite non-load-bearing light steel-framed walls are considered, depending on the type of protection layers and insulations and their position within the steel frame when subjected to elevated temperatures due to fire. The configuration cases are studied for a vertical panel from a compartment of an industrial building in Chlef designed by the FRAMEMETAL group, Figure 1.

Finite element models, using ANSYS APDL, are produced to predict the temperature profiles, maximum temperatures, and the estimated fire resistance level (FRL), taking into account the critical temperature as specified by EN 1993-1-2 [25] for members with Class 4 cross-sections. The influence of different systems of protection and insulation used for the CFS under fire conditions is evaluated.

2 LSF walls and configurations

LSF walls are made from two trucks and seven studs, evenly spaced by 630 mm, with a steel grade of G345, a density of 7850 kg/m³. The geometry details of CFS Lipped Channel (LC) members and dimensions of the frame are presented in Figure 2 and Table1.

The LSF is protected with 10 mm of different types of external protection and insulation in four configurations, with the aim of studying the influence of the layers of protection. Table 2 lists nine models of wall protection systems under consideration, and technical information about the adopted LSF system is described in the CNERIB document [31]. The first configuration considers three thermal protection models of LSF walls to be analyzed for each type, plasterboard, MGO, and cork with no insulation. The second configuration includes two models that incorporate MGO protection as well as cavity insulation of rockwool and glass fiber within the panel. The third configuration is taken on the basis of the second, with insulations positioned on both sides against LSF wall panels, forming a new composite system. The fourth configuration, considering two models, consists of an external insulation on the exposed side placed between MGO and plasterboard protections. Single plasterboard is used on the unexposed side. In this study, all configurations of LSF wall models are subjected to standard fire testing according to ISO 834.

Figure 1. Structure of light gauge steel panels (ONAPH building Chlef, Algeria)
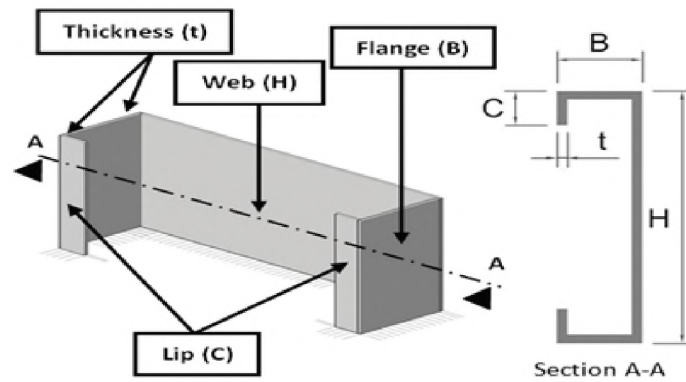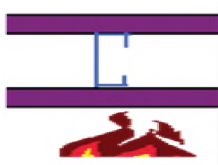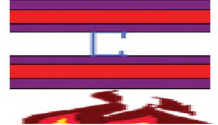
Figure 2. Geometry details of CFS members (LC H x B x C x t)

Table 1. Dimensions of CFS elements of the frame

Profiles	Dimensions				
	H (mm)	B (mm)	C (mm)	t (mm)	L (m)
Truck	152.4	50.8	No lips	1.37	4
Stud	152.4	41.15	12.7	1.37	3.7

Table 2. Details of configurations and models of protection

Configuration		Model	Type of Protection	Insulation
1		1	Plasterboard	No Insulation
		2	MGO	
		3	Cork	
2		4	MGO	Glass fibre (Cavity - 152.4 mm)
		5		Rockwool (Cavity - 152.4 mm)
3		6	MGO	Glass fibre (Sandwiched -75 mm)
		7		Rockwool (Sandwiched-75 mm)
4		8	MGO & Plasterboard (In exposed side) Plasterboard (In unexposed side)	Glass fibre (Sandwiched - 75 mm)
		9		Rockwool (Sandwiched - 75 mm)

3 Thermal properties and heat transfer action on partition LSF walls

3.1 Thermal properties

Thermal properties, conductivity, and specific heat of CFS, as provided by EN 1993-1-2 [25], are illustrated in Figure 3.

The LSF is protected with 10 mm of different types of external protection and insulation in four configurations, considering nine models of protection of wall systems. Thermal properties of the external protection, plasterboard (Figure 4(a)), magnesium oxide board (MGO) Figure 4(b) and cork (Figure 4(c)) are taken from studies developed by Sultan [32], Rusthi et al. [33], and Piloto et al. [34], respectively.
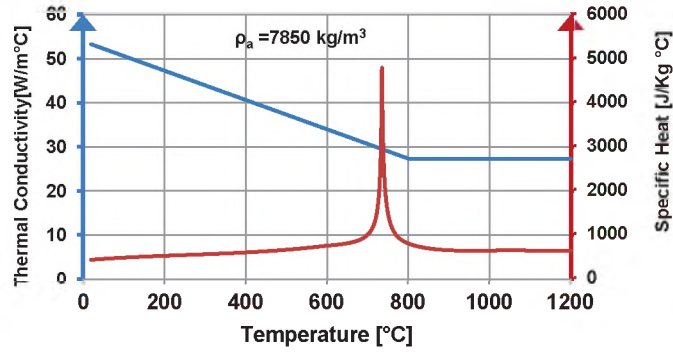
Figure 3. Steel conductivity & specific heat versus temperature
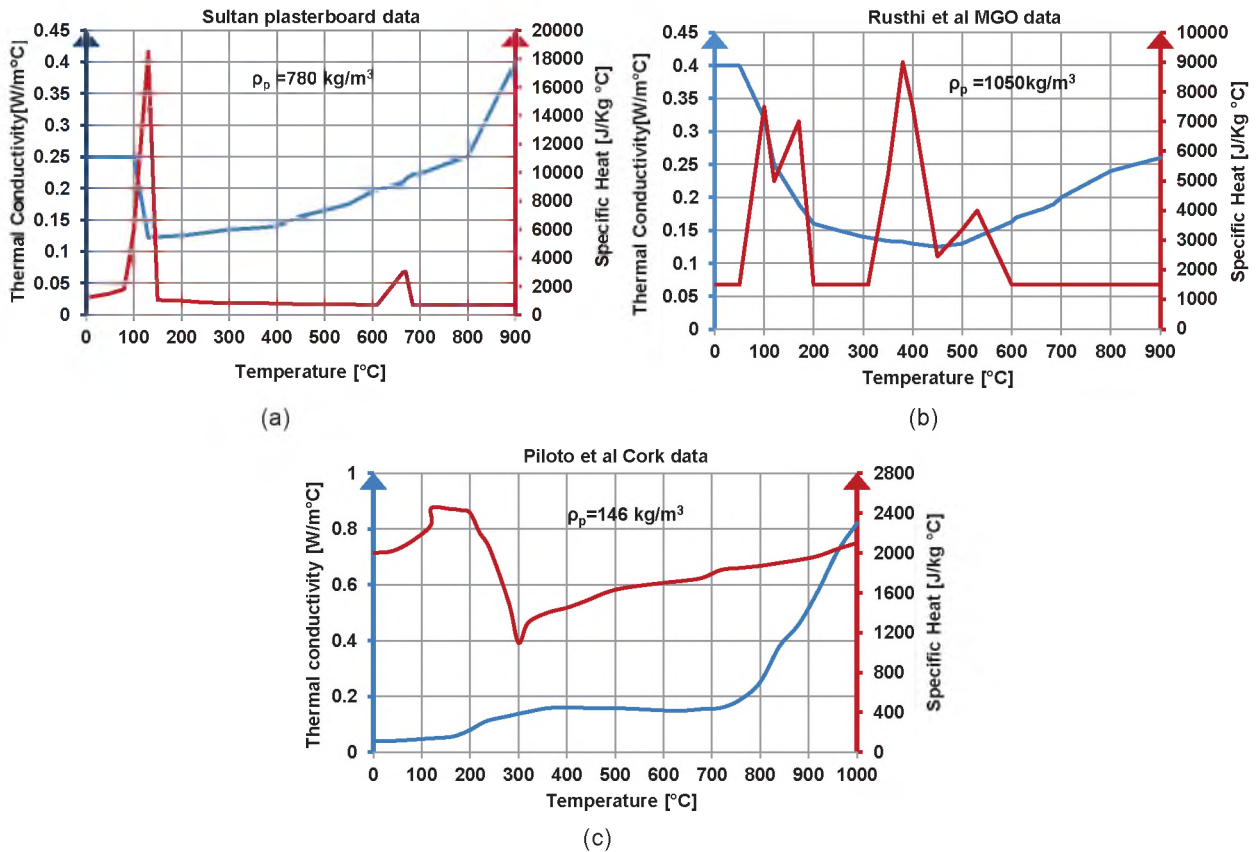

(a)

(b)

(c)

Figure 4. Thermal properties of external protection, (a) Plasterboard, (b) MGO, (c) Cork

The rockwool and glass fibre materials are used as cavity and external insulations. Their properties were obtained from the study of Lundberg [35] Figure 5(a), and Keerthan and Mahendran [24] Figure 5(b), respectively.
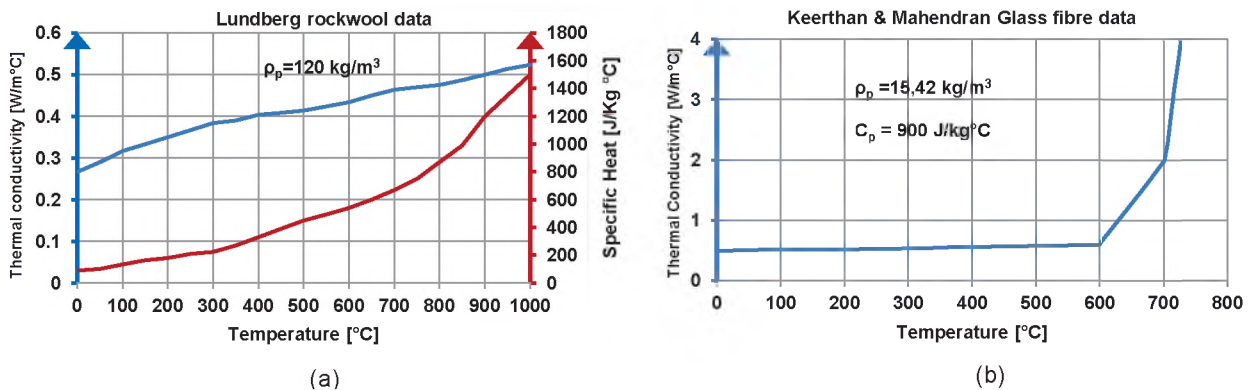

(a)

(b)

Figure 5. Thermal properties of cavity insulation, (a) Rockwool, (b) Glass fibre

3.2 Heat transfer action on partition LSF walls

The temperature profiles for LSF members are obtained from the nonlinear thermal analysis performed on ANSYS® [36] as a solution of conduction within the steel section governed by the Fourier equation [37], equation (1), using convection and radiation as boundary conditions.

$$\frac{\partial}{\partial x}\left(\lambda_a \frac{\partial \theta}{\partial x}\right) + \frac{\partial}{\partial y}\left(\lambda_a \frac{\partial \theta}{\partial y}\right) + \dot{Q} = \rho_a c_a \frac{\partial \theta}{\partial t} \qquad (1)$$

Where λ_a is the thermal conductivity, c_a is the specific heat of steel, ρ_a is the density of steel and $\dot{Q}$ is the energy source equal to zero in the case of a non-combustible element. The fire action is applied in the exposed faces of the materials of protection using ISO 834 equation (2), given in EN1993-1-2 [25].

$$\theta_g = 20 + 345 \log_{10}(8t + 1) \qquad (2)$$

Where θ_g is the gas temperature [°C] and t is the time [minutes].

The second solution for the non-linear equation (1) is the simplified method from EN1993-1-2 [25], considering an equivalent uniform temperature during a time interval Δt defined by equation (3a) and equation (3b) for unprotected and protected members, respectively.

$$\Delta\theta_{a,t} = k_{sh} \cdot (A_m / V) \cdot \dot{h}_{net,d} \Delta t / (c_a \cdot \rho_a) \qquad (3a)$$

$$\Delta\theta_{a,t} = \frac{\lambda_p \cdot A_p / V \cdot (\theta_g - \theta_m)}{d_p \cdot c_a \cdot \rho_a (1 + \phi/3)} \Delta t - (e^{\phi/3} - 1) \cdot \Delta\theta_{g,t} \qquad (3b)$$

Where k_{sh} is the correction factor for the shadow effect, A_m/V and A_p/V are the section factors for unprotected steel members and those insulated by fire protection material, respectively, λ_p, c_p, ρ_p and d_p are the thermal conductivity, specific heat, density, and thickness of the fire protection material, respectively, $\dot{h}_{net,d}$ is the design value of the net heat flux due to convection and radiation per unit area evaluated according to equation (4).

$$\dot{h}_{net,d} = \alpha_c(\theta_g - \theta_m) + \phi \varepsilon_r \sigma \left[(\theta_g + 273)^4 - (\theta_m + 273)^4\right] \qquad (4)$$

Where α_c is the convection heat transfer coefficient, $\varepsilon_r = \varepsilon_f \varepsilon_m$ with ε_r the emissivity coefficient of the surface of the element equal to 0.7 and ε_f equal to 1 in case of fire, σ is constant of Stefan–Boltzmann ($\sigma = 5.67 \times 10^{-8}$ W/m^2·K^4), θ_m is the surface element temperature, and θ_g is the gas temperature, ϕ is the configuration factor equal to 1 for

unprotected members and obtained according to equation (5) for protected members.

$$\phi = \frac{c_p \cdot \rho_p}{c_a \cdot \rho_a} \cdot d_p \cdot A_p / V \qquad (5)$$

4 Thermal analysis models

This part describes the thermal finite element models used for all simulations performed for LSF walls in order to investigate their thermal response and predict their temperature profiles, maximum temperatures, and fire resistance level (FRL). Appropriate mesh is adopted, and thermal boundary conditions of convection and radiation are applied for CFS elements and protection materials.

4.1 Thermal FE models

Finite element analyses were conducted under transient and nonlinear thermal analyses, based on SHELL131 and SOLID70 elements for CFS members and external protections and insulations, respectively. The contact between solids and shells is considered perfect. Figure 6 shows the geometry and the topology of these finite elements. The latter are used with linear interpolating functions and full integration methods from ANSYS® [36]. SHELL 131 has four nodes with up to 32 degrees of freedom at each node. It is a three-dimensional layered shell element with in-plane and through-thickness thermal conduction capability that is suitable for transient thermal analysis. SOLID 70 has eight nodes and a single degree of freedom, temperature, at each node applicable to a 3-D, steady-state, or transient thermal analysis.

4.2 Mesh and boundary conditions

The thermal model is meshed by shell and solid finite elements with size of 20 × 50 mm for the web and flanges, and a size of 20 × 20 mm around the circular hole region, with the lip being one single element as shown in Figure 7.

The ISO834 is applied as bulk temperature on the exposed side of the wall according to EN-1991-1-2 [38], with heat transfer by convection having a coefficient of 25 W/m²K. The unexposed side is considered ambient with an applied boundary condition of convection and a film coefficient of 9 W/m²K which include the radiation effect. For the models without cavity insulation, the same boundary conditions are applied, but according to Gunalan [39] an extra radiation is applied to an empty cavity with an emissivity coefficient equal to 0.9 at the cavity surface.
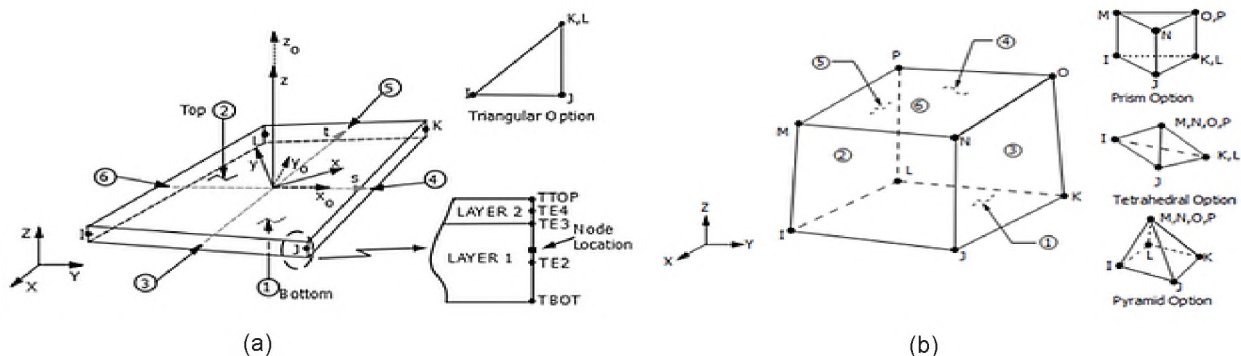

(a)   (b)

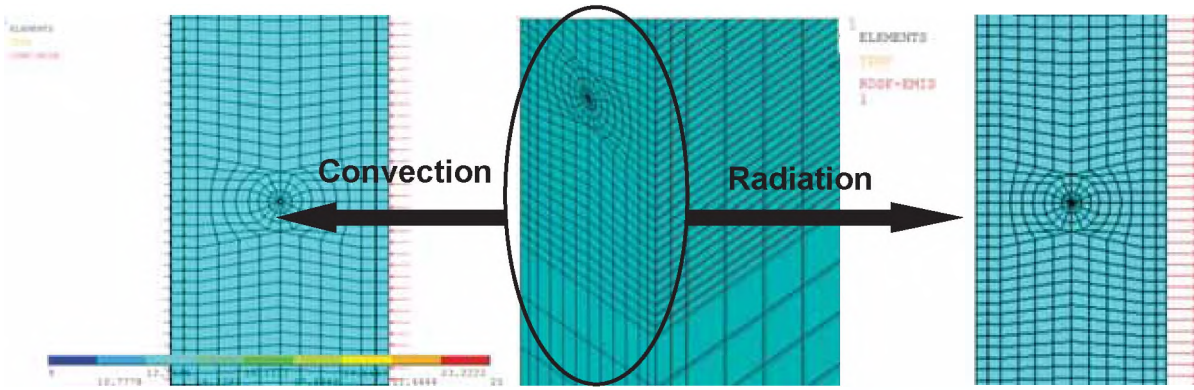*Figure 6. Geometry & topology of finite element models, (a) SHELL131, (b) SOLID70 [36]*

Figure 7. Meshing of the model and Boundary conditions

4.3   Model validation

In this section, a validation of thermal FE models is presented and compared with the fire test result obtained by Rusthi, et al. [33] for the LSF wall system. The test was conducted with 3.15 m × 3.15 m LSF panel of six stiffened channel studs (LC 92 × 35 × 15 × 1.15 mm) equally spaced by 600 mm, and fixed between two tracks at the top and the bottom, and then lined with 10 mm thick of MGO. Figure 8 shows the thermocouples position during the test from which average temperature curves for stud flanges were extracted.

The average temperature evolution of the hot flange (HF) and the cold flange (CF) are presented in Figure 9. The latter shows the comparison between the results of the experimental study and the numerical simulation obtained from the numerical model and highlights a good agreement in temperature profiles within the sections.

5   Results and discussion

Results from simulations produce temperature contours, time-temperature evolution, and fire resistance levels for all configurations in order to investigate the thermal response of the LSF wall and study the effect of different protection materials. The temperature is extracted at the mid-height of the flanges of the middle stud, which are highly exposed to heat on both sides. The temperature evolution for the first configuration is presented for the three thermal models in Figure 10.

It can be observed that a maximum temperature of 564 °C in HF and 458 °C in CF can be reached for model 2 based on the MGO board, which is much lower than those of models 1 and 3. While the model 2 with the MGO board had a slow rise in temperature, the model 3 with the cork lined panel had a rapid rise in temperature. For the later model, the highest temperature in HF is reached for at a maximum
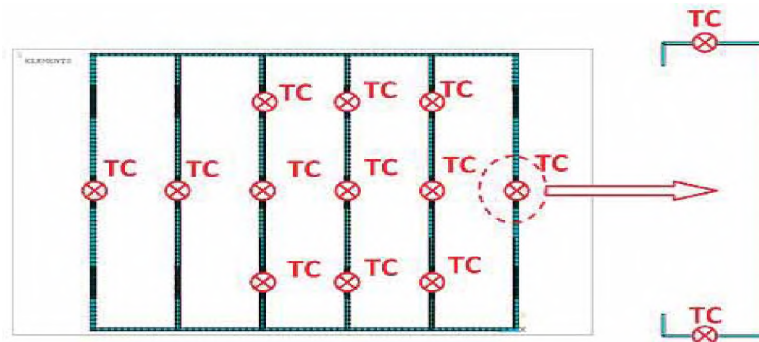

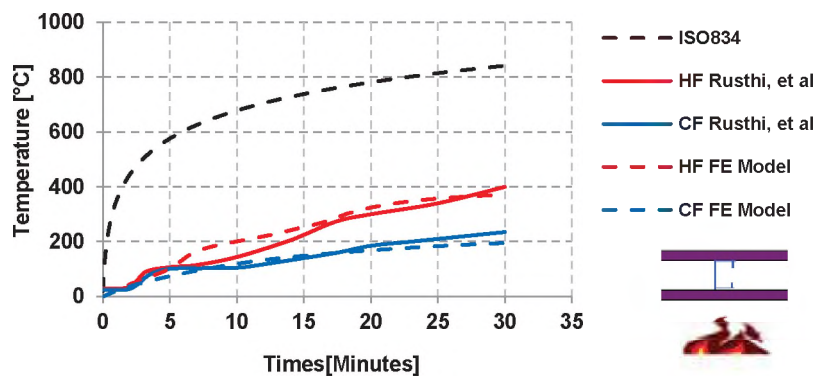*Figure 8. Thermocouple locations on studs [33]*

Figure 9. Average temperature evolution of LSF wall from tests and thermal FE analyses
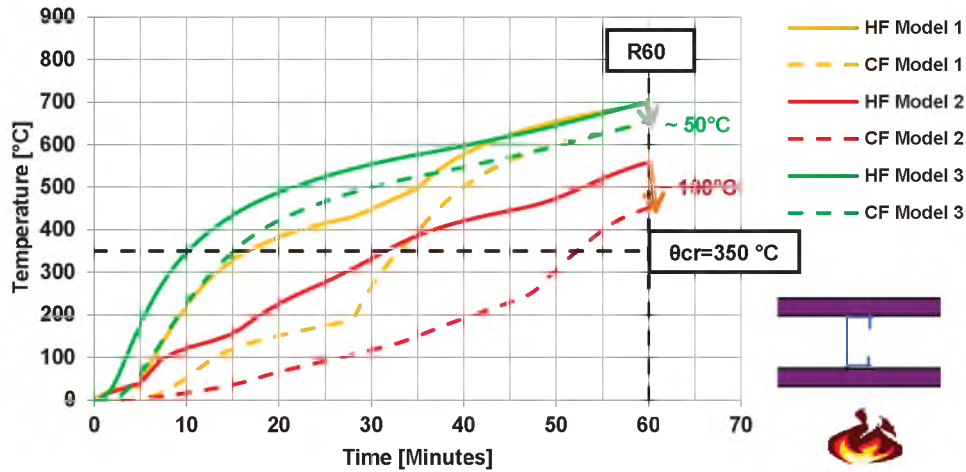
Figure 10. Temperature evolution at mid-height stud of LSF wall (Configuration 1)

of 707 °C, with a temperature difference of 50°C between HF and CF after 60 minutes. Figure 11 shows the temperature contours of the thermal model 2 at 60 minutes.

The second configuration, which comprises thermal models 4 and 5, aims to investigate the effect of the position of cavity insulations within the panel on improving the fire resistance. The temperature evolution shown in Figure 12 shows that the thermal model 4 based on glass fibre insulation has reached a maximum temperature of 732 °C and 188 °C in stud HF and CF, respectively, at 60 minutes.

These temperatures are higher compared to those provided by model 5 based on rockwool insulation, and the temperature difference between HF and CF for models 4 and 5 is 544°C and 620 °C, respectively. Therefore, the presence of the cavity insulation within the panel reduces the heat transfer through the stud cold flange, and leads to a rapid increase in temperature in the stud hot flange. It can be seen that temperatures in HF are higher than the critical temperature, resulting in the failure of studs in the case of a load-bearing wall.
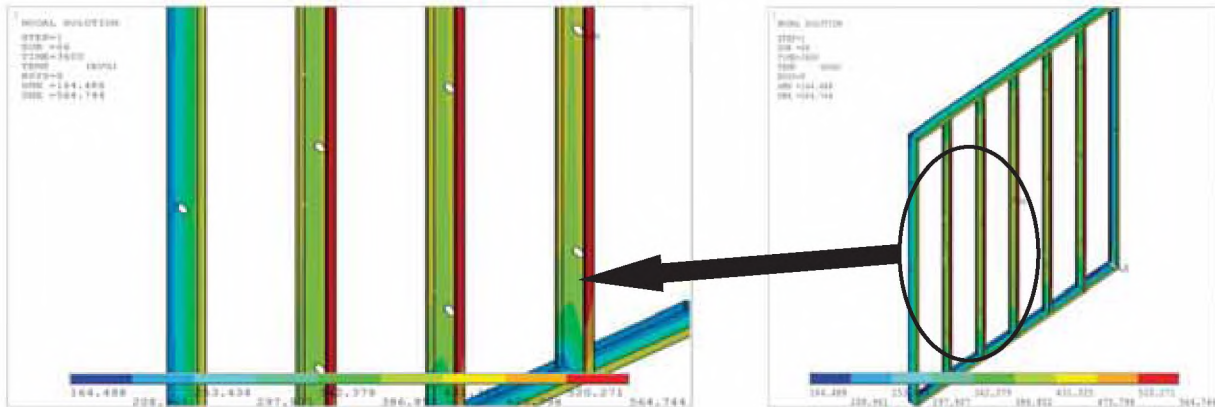

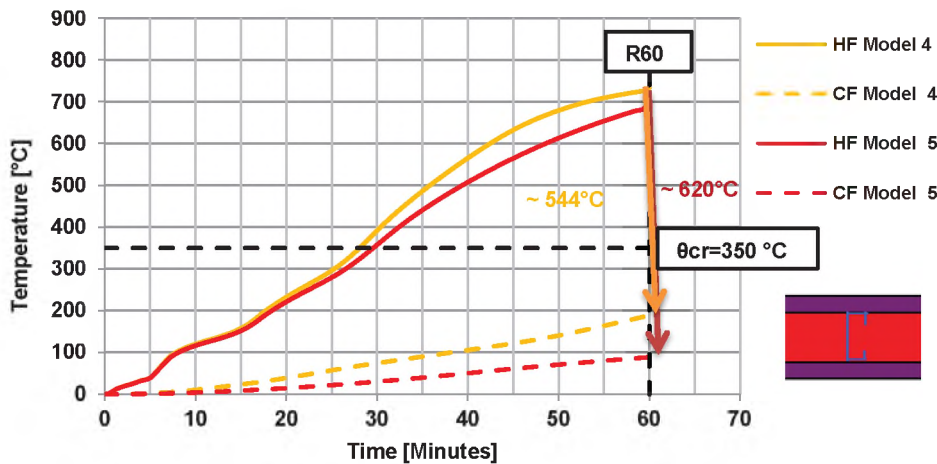Figure 11. Temperature contours of model 2 at 60 minutes

Figure 12. Temperature evolution at mid-height stud of composite LSF (Configuration 2)

Figure 13 shows temperature contours of the thermal model 5 at 60 minutes.

Figure 14 presents the temperature evolution for the third configuration, including the thermal models 6 and 7, which comprise the new composite LSF wall. Temperature progress is slow, with small temperature differences of 64 °C and 22 °C between the studs HF and CF for models 6 and 7, respectively. The maximum temperature does not exceed 120 °C at 60 minutes. The new composite wall system provides better fire performance compared to the traditional LSF wall, either with or without cavity insulation, used in configurations 1 and 2.

Figure 15 shows temperature contours of the thermal model 7 at 60 minutes.

Figure 16 presents results for the temperature evolution of the fourth configurations of models 8 and 9. The temperature difference between HF and CF, the maximum temperature, and the temperature evolution are comparable to those of the third configuration, with slight differences in results.

Figure 17 shows temperature contours of the model 9 at 60 minutes.
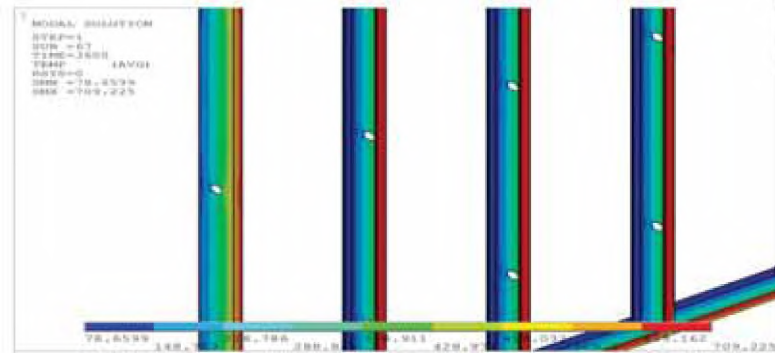

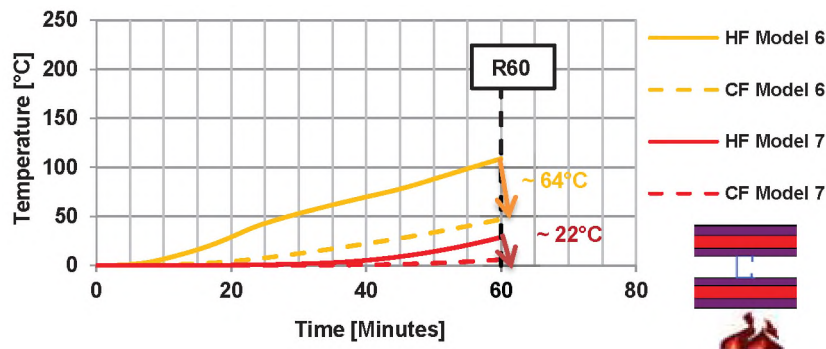*Figure 13. Temperature contours of model 5 at 60 minutes*

Figure 14. Temperature evolution at mid-height stud of new composite LSF wall (Configuration 3)
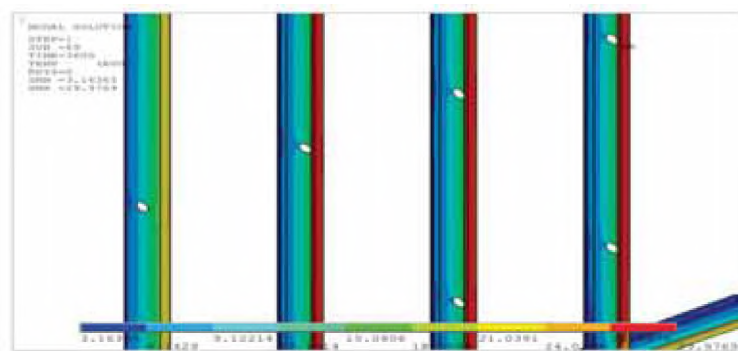

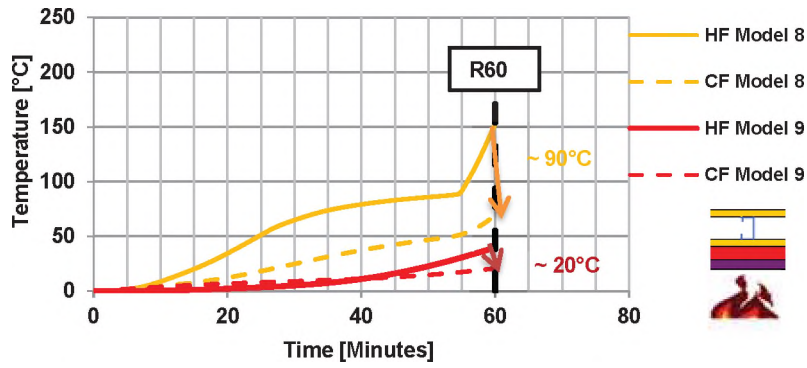*Figure 15. Temperature contours of model 7 at 60 minutes*

Figure 16. Temperature evolution at mid-height stud of proposed LSF (Configuration 4)
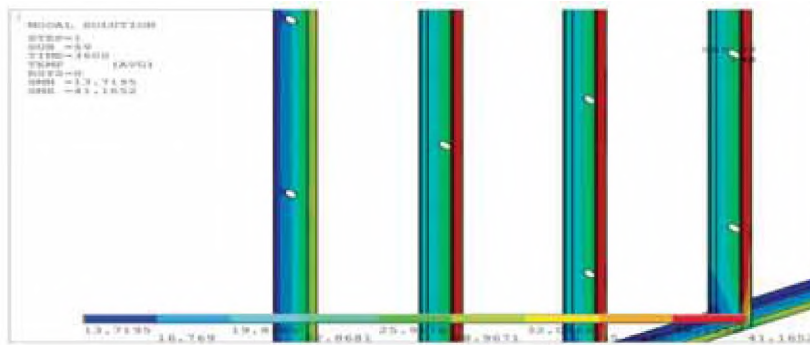

Figure 17. Temperature contours of model 9 at 60 minutes

Table 3 summarizes all the results obtained for all configurations for maximum temperatures, at mid-height of the flanges HF and CF of the most exposed stud at 60 minute.

Table 4 shows the failure time for all thermal models at the critical temperature of 350 °C as specified in EN 1993-1-2 [25], to obtain the fire resistance level (FRL) for each model.

Table 4 shows that the model 2 based on MGO board achieved the highest FRL with a failure time of 31 minutes, which is significantly better than the FRL from models of configuration 1, with failure time differences of 15 minutes for

plasterboard and 20 minutes for cork. The position of cavity insulation within the panel produces approximately the same FRL as obtained from Model 2. In the presence of rockwool and glass fiber insulation, the temperature in HF rapidly rises above the critical temperature. It is observed that the failure time has not been reached for configurations 3 and 4. The FRL could be improved by using insulation externally sandwiched between two layers of protection. The temperature contours of the most exposed middle stud of all panels lined with MGO at the failure time are presented in Figure 18.

Table 3. Maximum temperatures at mid-height of the middle stud

Configuration	Model	Temperature [°C] (at 60 minutes)	
		CF	HF
1	1	650	699
	2	458	564
	3	655	707
2	4	188	732
	5	88	709
3	6	47	111
	7	7	29
4	8	70	159
	9	21	41

Table 4. Fire resistance level (FRL) of non-load bearing LSF walls

Configuration	Model	Fire resistance level (FRL) [Min] (Critical temperature of 350°C, EC3-1-2)
1	1	16
	2	31
	3	10
2	4	28
	5	29
3	6	>60
	7	>60
4	8	>60
	9	>60

(a) *Model 2*   (b) *Model 4*   (c) *Model 5*
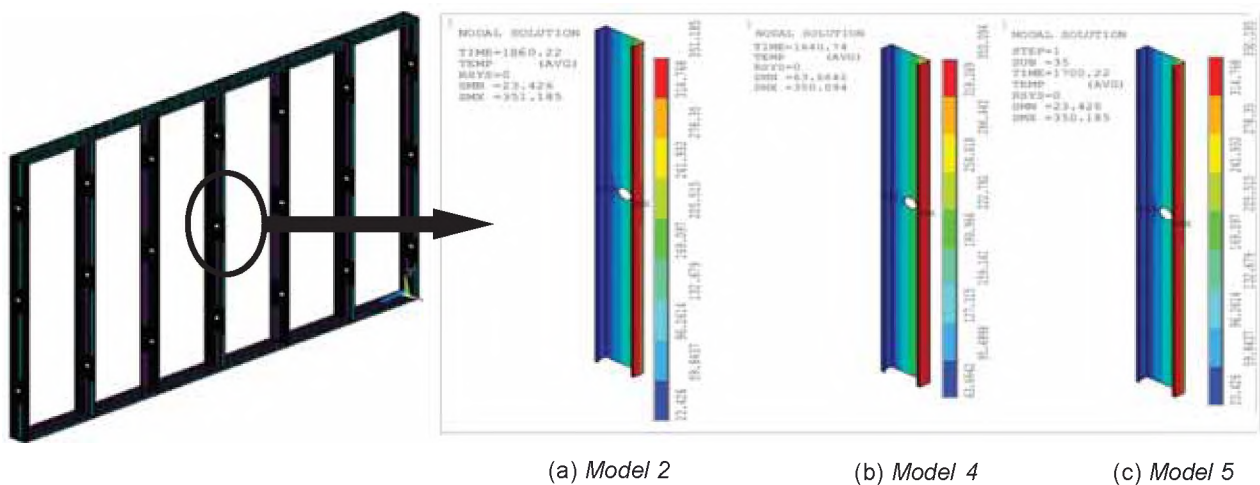
Figure 18. Temperature contours at the failure time of panels lined with MGO

6   Conclusions

A numerical investigation based on the validated finite element model of the thermal response of the LSF wall system under fire, ISO 834, is presented, considering the effect of different protections. The thermal transient analysis with the full option solution method was performed using ANSYS APDL. The numerical heat transfer results of the LSF wall configurations include a time–temperature curve and temperature contours, which are used to study the influence of different systems of protection and insulation on improving the fire resistance. The analysis shows predicted temperatures and fire resistance levels for different configurations, and the following conclusions are drawn:

• In configuration 1, the temperature of 564 °C obtained from stud HF of the protected panel by magnesium oxide board is lower than those of plasterboard and cork, which are 699 °C and 707 °C, respectively.

• Considering the critical temperature of 350 °C specified by EC3, the MGO board leads to an increase in the failure time in comparison with the other two protections by providing a fire resistance level (FRL) of 31 minutes which is much better than the FRLs of plasterboard and cork of 16 minutes and 10 minutes, respectively.

• The presence of cavity insulation within the panel reduces the heat transfer across the stud cold flange, and leads to a rapid increase in temperature in the stud hot flange. This may cause the early failure of the overall panel in the case of a load-bearing wall.

• The failure time of configuration 2 (panels protected by MGO with an insulation cavity) is about the same as configuration 1 (panels protected by MGO without an insulation cavity) at 29 minutes.

• The use of external insulation between two layers of protection forming a composite panel, (configuration 3), presents a higher thermal performance compared to the traditional LSF with/without cavity insulation with more than 60 minutes of FRL.

• The temperatures were very similar in both cases of LSF wall configurations 3 and 4. As a result, configuration 4, with a single sheet of plasterboard on the exposed side and insulation between MGO and plasterboard on the unexposed side, offers a more cost-effective solution for the same thermal performance. Therefore, configuration 4 with a reduced protection system leads to a gain in work time and makes the structure lighter.

Acknowledgments

List of symbols

t	Time, [minutes]
C_a, λ_a, ρ_a	Specific heat [J/kg°C], thermal conductivity [W/m°C] and density [kg/m^3] of steel, respectively.
C_p, λ_p, ρ_p, d_p	Specific heat [J/kg°C], thermal conductivity [W/m°C], density [kg/m^3] and thickness of protection materials [mm], respectively.
k_{sh}	Correction factor for shadow effect
E	Modulus of elasticity, N/mm^2
f_y	Yield strength, N/mm^2
$\dot{h}_{net,d}$	Design value of the net heat flux, w/m²
$\dot{Q}$	Energy source
θ_g	Gas temperature in the fire compartment, °C
θ_m	Temperature of the member surface, °C
α_c	Convection heat transfer coefficient, W/m^{2}K
ε_f ε_m	Emissivity coefficient,
ϕ	Configuration factor,
σ	Constant of Stefan–Boltzmann, W/m^2·K^4
v	Poisson's ratio

Subscripts

CFS	Cold Formed Section
LSF	Light gauge Steel Framed
MGO	Magnesium Oxide board
HF	Hot Flange
CF	Cold Flange
TC	Thermocouple

References

[1] Liang, H., Roy, K., Fang, Z., and Lim, J. B., A critical review on optimization of cold-formed steel members for better structural and thermal performances, Buildings, vol. 12,(2022), 12-34. https://doi.org/10.3390/buildings12010034

[2] Jakovljević, I., Dobrić, J., and Marković, Z., Flexural buckling of hot-finished and cold-formed elliptical hollow section columns: Numerical comparative analysis, Građevinski materijali i konstrukcije, vol. 62,(2019), 15-32. https://doi.org/10.5937/GRMK1902015J

[3] Kada, A., Lamri, B., Mesquita, L., and Bouchair, A., Finite element analysis of steel beams with web apertures under fire condition, Asian Journal Of Civil Engineering (Building And Housing), vol. 17,(2016), 1035-1054.

[4] Laím, L., Rodrigues, J. P. C., and da Silva, L. S., Experimental analysis on cold-formed steel beams subjected to fire, Thin-Walled Structures, vol. 74,(2014), 104-117. https://doi.org/10.1016/j.tws.2013.09.006

[5] Laban, M. Đ., Radonjanin, V. S., Malešev, M. M., and Radeka, M. M., Construction products performances and basic requirements for fire safety of facades in energy rehabilitation of buildings, Tehnika, vol. 70,(2015), 759-766. https://doi.org/10.5937/tehnika1505759L

[6] Benyettou Oribi, S., Kada, A., Lamri, B., and Mesquita, L. M., Investigation of residual stresses on the fire resistance of unrestrained cellular beams, ce/papers, vol. 4,(2021), 1386-1394. https://doi.org/10.1002/cepa.1436

[7] Kada, A. and Lamri, B., Numerical analysis of non-restrained long-span steel beams at high temperatures due to fire, Asian Journal of Civil Engineering, vol. 20,(2019), 261-267. https://doi.org/10.1007/s42107-018-0103-7

[8] Merouani, M. R., Lamri, B., Kada, A., and Piloto, P., Mechanical analysis of a portal steel frame when subjected to a post-earthquake fire, Fire Research, vol. 3,(2019), 38-43. https://doi.org/10.4081/fire.2019.76

[9] Mesquita, L., Piloto, P., Vaz, M., and Vila Real, P., Experimental and numerical research on the critical temperature of laterally unrestrained steel I beams, Journal of Constructional Steel Research, vol. 61,(2005), 1435-1446. https://doi.org/10.1016/j.jcsr.2005.04.003

[10] Nadjai, A., Petrou, K., Han, S., and Ali, F., Performance of unprotected and protected cellular beams in fire conditions, Construction and Building Materials, vol. 105,(2016), 579-588. https://doi.org/10.1016/j.conbuildmat.2015.12.150

[11] Bailey, C., Indicative fire tests to investigate the behaviour of cellular beams protected with intumescent coatings, Fire safety journal, vol. 39,(2004), 689-709. https://doi.org/10.1016/j.firesaf.2004.06.007

[12] Lamri, B., Mesquita, L., Abdelhak, K., and Piloto, P., Behavior of cellular beams protected with intumescent coatings, Fire Research, vol. 1,(2016), 27-32. https://doi.org/10.4081/fire.2017.27

[13] Mesquita, L., Gonçalves, J., Gonçalves, G., Piloto, P., and Kada, A. Intumescente fire protection of cellular beams, X Congresso de Construção Metálica e Mista, Coimbra, Portugal,(2015).

[14] Chen, W., Jiang, J., Ye, J., Zhao, Q., Liu, K., and Xu, C., Thermal behavior of external-insulated cold-formed steel non-load-bearing walls exposed to different fire conditions, Structures, vol. 25,(2020), 631-645. https://doi.org/10.1016/j.istruc.2020.03.044

[15] Ariyanayagam, A., Poologanathan, K., and Mahendran, M., Thermal modelling of load bearing cold-formed steel frame walls under realistic design fire conditions, Advanced Steel Construction, vol. 13,(2017), 160-189. https://doi.org/10.18057/ijasc.2017.13.2.5

[16] Balachandren, B., Numerical and experimental studies of cold-formed steel floor systems under standard fire conditions, PhD Thesis, Queensland University of Technology, (2012).

[17] Piloto, A. G. P., Khetata, S. M., and Gavilán, B. R. A., Fire performance of non-loadbearing light steel framing walls – numerical and simple calculation methods, MATTER: International Journal of Science and Technology, vol. 3,(2017), 13-23. https://doi.org/10.20319/mijst.2017.32.1323

[18] Piloto, P. Light steel framed walls made with composite panels under fire conditions, 6th Conference on Urban Fire Safety and 1st Civil Protection Conference, Universidade de Coimbra- Portugal (2018).

[19] Rusthi, M. I., Experimental and finite element studies of light-gauge steel frame wall systems under fire conditions, PhD Thesis, Science and Engineering Faculty, Queensland University of Technology, (2017).

[20] Chen, W., Ye, J., and Zhao, Q., Thermal performance of non-load-bearing cold-formed steel walls under different design fire conditions, Thin-Walled Structures, vol. 143,(2019), 106-242. https://doi.org/10.1016/j.tws.2019.106242

[21] Kolarkar, P. N., Structural and thermal performance of cold-formed steel stud wall systems under fire conditions, PhD Thesis, School of urban development, Queensland University of Technology, Australia, (2010).

[22] Kolarkar, P. and Mahendran, M., Experimental studies of non-load bearing steel wall systems under fire conditions, Fire safety journal, vol. 53,(2012), 85-104. https://doi.org/10.1016/j.firesaf.2012.06.009

[23] Baleshan, B. and Mahendran, M., Numerical study of high strength LSF floor systems in fire, Thin-Walled Structures, vol. 101,(2016), 85-99. https://doi.org/10.1016/j.tws.2015.12.018

[24] Keerthan, P. and Mahendran, M., Thermal performance of composite panels under fire conditions using numerical studies: plasterboards, rockwool, glass fibre and cellulose insulations, Fire Technology, vol. 49,(2013), 329-356. https://doi.org/10.1007/s10694-012-0269-6

[25] EN1993-1-2, Eurocode 3: Design of steel structures - Part 1-2: General rules - Structural fire design [Authority: The European Union Per Regulation 305/2011, Directive 98/34/EC, Directive 2004/18/EC], 2005), 78.

[26] Ariyanayagam, A. D. and Mahendran, M., Fire tests of non-load bearing light gauge steel frame walls lined with calcium silicate boards and gypsum plasterboards, Thin-Walled Structures, vol. 115,(2017), 86-99. https://doi.org/10.1016/j.tws.2017.02.005

[27] Ariyanayagam, A. D. and Mahendran, M., Influence of cavity insulation on the fire resistance of light gauge steel framed walls, Construction and Building Materials, vol. 203,(2019), 687-710. https://doi.org/10.1016/j.conbuildmat.2019.01.076

[28] Khetata, S. M., Piloto, P. A., and Gavilán, A. B., Fire resistance of composite non-load bearing light steel framing walls, Journal of Fire Sciences, vol. 38,(2020), 136-155. https://doi.org/10.1177/0734904119900931

[29] Rajanayagam, H., Upasiri, I., Poologanathan, K., Gatheeshgar, P., Sherlock, P., Konthesingha, C., Nagaratnam, B., and Perera, D., Thermal Performance of LSF Wall Systems with Vacuum Insulation Panels, Buildings, vol. 11,(2021), 621. https://doi.org/10.3390/buildings11120621

[30] Rahnavard, R., Craveiro, H. D., Simões, R. A., and Santiago, A., Equivalent temperature prediction for concrete-filled cold-formed steel (CF-CFS) built-up column sections (part A), Case Studies in Thermal Engineering, vol. 33,(2022), 101928. https://doi.org/10.1016/j.csite.2022.101928

[31] C.N.E.R.I.B, Avis sur système constructif LIGHT GAUGE STEEL, FRAMEMETAL, Avis Technique 2, 2016.

[32] Sultan, M. A., A model for predicting heat transfer through noninsulated unloaded steel-stud gypsum board wall assemblies exposed to fire, Fire Technology, vol. 32,(1996), 239-259. https://doi.org/10.1007/BF01040217

[33] Rusthi, M., Ariyanayagam, A., Mahendran, M., and Keerthan, P., Fire tests of Magnesium Oxide board lined light gauge steel frame wall systems, Fire safety journal, vol. 90,(2017), 15-27. https://doi.org/10.1016/j.firesaf.2017.03.004

[34] Piloto, P., Khetata, M., and Gavilán, A. B. Fire resistance of non-loadbearing LSF walls, 2nd Conference on Testing and Experimentations in Civil Engineering, Porto, Portugal,(2019).

[35] Lundberg, S., Material Aspects of Fire Design, TALAT Lectures 2502,(1994). https://www.slideshare.net/corematerials/talat-lecture-2502-material-aspects-of-fire-design (accessed 17 July 2021).

[36] ANSYS®, Academic Research, Release 16.2: ANSYS, Canonsburg, PA, USA, 2015.

[37] Franssen, J.-M. and Vila Real, P., Fire Design of Steel Structures: Eurocode 1: Actions on structures; Part 1-2: General actions--Actions on structures exposed to fire; Eurocode 3: Design of steel structures; Part 1-2: General rules--Structural fire designJohn Wiley & Sons,2012.

[38] EN-1991-1-2, Eurocode 1: Actions on structures—Part 1-2: General actions—Actions on structures exposed to fire [Authority: The European Union Per Regulation 305/2011, Directive 98/34/EC, Directive 2004/18/EC], British Standards, 2002), 58.

[39] Gunalan, S., Structural behaviour and design of cold-formed steel wall systems under fire conditions, PhD thesis, Faculty of built environment and engineering, Queensland University of Technology, (2011).